RESISTIVE SENSOR FOR SHORT HPM PULSE MEASUREMENT

(Final report)

A. Goštauto 11, Vilnius 2600, Lithuania
Tel.: 3702 619808
Fax: 3702 627123

E-mail: kancleris@uj.pfi.lt

Vilnius, 1998

REPORT DOCUMENTATION PAGE

Form Approved OMB No. 0704-0188

1. AGENCY USE ONLY (Leave blank)	2. REPORT DATE	3. REPORT TYPE AND DATES COVERED
	Dec. 1998	Final Report

4. TITLE AND SUBTITLE

Resistive Sensor for Short HPM Pulse Measurement

5. FUNDING NUMBERS

F6170897W0208

6. AUTHOR(S)

Dr. Zilvinas Kancleris

7. PERFORMING ORGANIZATION NAME(S) AND ADDRESS(ES)

Semiconductor Physics Institute
Microwave Laboratory
A. Gostauto 11
Vilnius 2600
Lithuania

8. PERFORMING ORGANIZATION REPORT NUMBER

N/A

9. SPONSORING/MONITORING AGENCY NAME(S) AND ADDRESS(ES)

EOARD
PSC 802 BOX 14
FPO 09499-0200

10. SPONSORING/MONITORING AGENCY REPORT NUMBER

SPC 97-4050

11. SUPPLEMENTARY NOTES

12a. DISTRIBUTION/AVAILABILITY STATEMENT

Approved for public release; distribution is unlimited.

12b. DISTRIBUTION CODE

A

13. ABSTRACT (Maximum 200 words)

This report results from a contract tasking Semiconductor Physics Institute as follows: The contractor will investigate the development of a resistive sensor for HPM pulse measurement. Contractor will work on improving the rise time of the sensor and optimizing the frequency response and will design and manufacture sensors as described in the proposal.

14. SUBJECT TERMS

EOARD, sensors, Pulsed Power

15. NUMBER OF PAGES

26

16. PRICE CODE

N/A

17. SECURITY CLASSIFICATION OF REPORT	18. SECURITY CLASSIFICATION OF THIS PAGE	19. SECURITY CLASSIFICATION OF ABSTRACT	20. LIMITATION OF ABSTRACT
UNCLASSIFIED	UNCLASSIFIED	UNCLASSIFIED	UL

Contents

Introduction

The present report consists of introduction, 3 chapters, conclusions and appendixes. In the first chapter the performance of the resistive sensor is described. The setups used for time and frequency response investigation and calibration are presented in this chapter. In the next chapter the DC pulse adapter used for the resistive sensor feeding is described. In the third chapter main characteristics of the resistive sensors are given. In the Appendixes the results of the tests of the resistive sensors at a few laboratories in the USA are collected. Hereinafter we used abbreviation RS to signify the resistive sensor. The term sensor is used to denote the sensing element of the RS.

The aim of the present work was to design and fabricate the RS that can be used for high power microwave (HPM) pulse measurement. We also investigate the response time of the RS and their frequency response.

The RS have been designed as a short section of particular waveguide where the sensor is placed. The frequency bands, waveguide dimensions, maximum calibration power and other technical characteristics have been fixed with customers and are listed in Table 1.

Table 1. Technical characteristics of the RS.

Band	Freq. Range GHz	Waveguide dimensions mm²	Waveguide flange type	Maximum calibration power kW	Maximum pulse duration ns	Pieces
L	1.1 ... 1.4	165.1 x 82.5	CPR 650	-[1]	300	2
S	2.8...3.0	72.1 x 34	CPR 284	100	100	2
C	4.0...5.0	47.65 x 22.15	WR 187	60	100	2
X	8.8...9.6	23 x 10	UG 135	100	200	4

1. Resistive sensor

Performance of the RS

The RS is a short section of the standard waveguide where a sensor that converts the microwave pulse to the DC pulse is placed. The sensor is a piece of n-type Si with Ohmic contacts on the ends. It is connected to a current source. The electric field of the electromagnetic wave heats electrons in a semiconductor, its resistance changes, and a DC pulse appears in the output. The amplitude of the pulse can be expressed as follows:

$$U_S = U_{DC}\varphi(E), \qquad (1.1)$$

where U_{DC} is the DC voltage drop across the sensor, E is the electric field strength averaged within the active element and $\varphi(E)$ is the relative resistance change of the semiconductor due to the

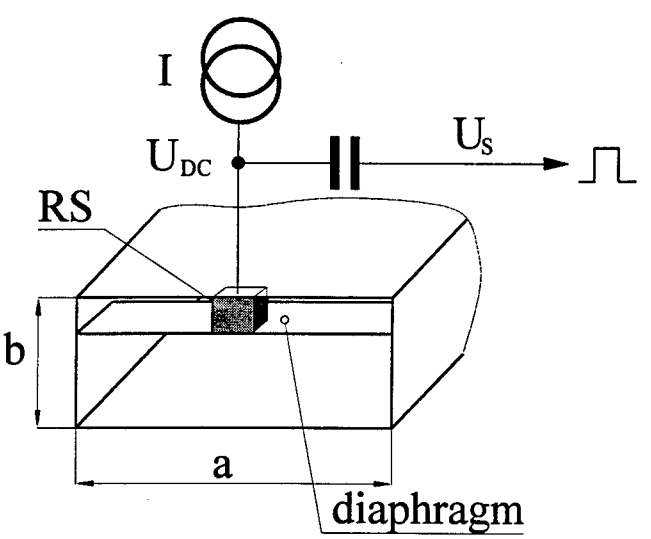

Figure 1. A cross section view of the RS for short HPM pulse measurement.

[1] *Suitable L-band source for the RS calibration is not available in the laboratory.*

electron heating effect. Since the average electric field strength depends on the microwave power, thus by measuring U_S the microwave pulse power in the transmission line can be determined.

For short HPM pulse measurement the diaphragm type RS shown in Figure 1 is usually used. It is seen that the sensor is placed between the thin metal foil and a wide wall of the waveguide. Its height corresponds roughly to 1/10 of the waveguide narrow wall. Such design allows to decrease average heating of the sensor and improve the other characteristics of the RS.

As follows from expression (1.1), the output signal of the RS increases linearly with the DC voltage applied to it. In order to increase the output signal and provide average sensor heating at sufficiently low level, the DC pulse supply is used. Using 50 V pulses for the sensor supply, the output signal of a few tens of volts can be obtained without any amplification [1]. The description of the unit that produces DC pulse for RS feeding is presented in chapter 3.

Measurement of the signal and calibration

The block diagram of the employed measurement circuit is shown in Figure 2. The synchronizing master generator switches the unit that produces DC pulses for the RS feeding. It outputs the DC pulse which duration and amplitude are roughly 180 μs and 50 V. The triggering pulse delayed nearly 150 μs starts high power microwave generator, so the duration of the microwave pulse is covered by the feeding pulse. When the microwave pulse reaches the RS its resistance increases and a DC pulse the duration of which corresponds to the duration of microwave pulse appears. The coil inductance in the splitting circuit is chosen in that way, that it has a low resistance for feeding pulse and a high resistance for the measuring one. Therefore, the output signal appears as a short video pulse on the pad of feeding pulse. The capacitor in the splitting circuit cuts off the pad and the short video pulse is detected by scope. Reference pulse power meter is connected to the main guide via directional coupler. As a reference power meter serves Rohde&Schwarz average power meter NRVS with thermocouple power sensor NRV-Z54. By measuring average power generated by HPM source and knowing pulse duration and repetition rate pulse power in the main guide is determined. For X-band we also used the

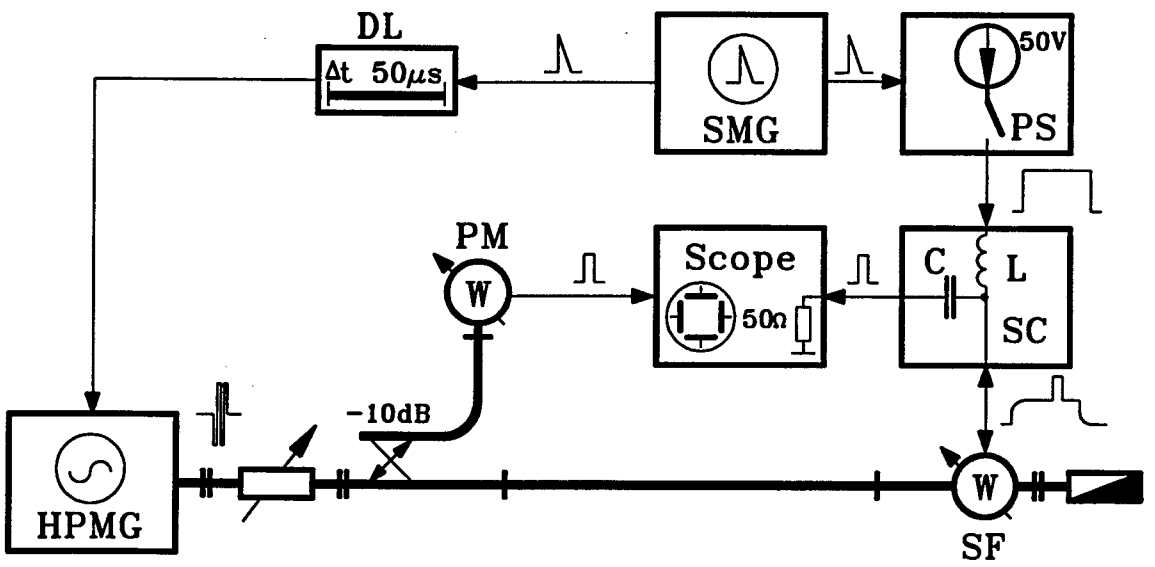

Figure 2. Experimental setup for short HPM pulse amplitude measurement using DC pulse supply: SMG: synchronizing master generator, DL: pulse delay line, PS: DC pulse supply, SC: splitting circuit, PM: reference pulse power meter, HPMG: high power microwave generator, SF: the RS under test.

pulse power meter where the other type of RS is employed. The pulse power meter is independently calibrated and compared with pulse power standard of Russia.

Response time investigation

Electron heating inertia is the physical reason that limits the response time of the RS. It is very fast process with the characteristic time of $2.9 \cdot 10^{-12}$ s for n-type Si at a room temperature. Therefore the actual response time of the sensor is determined by the pulse rise time in the DC circuit. Having no possibility to determine the response time directly using microwave pulse with short rise time we used the time domain reflectometry method the setup of which is shown in Figure 3.

50 Ω impedance pulse generator consisted of a pulse-forming line and mercury-wetted relay produces pulses 100 ns duration with rise time 0.05 ns. The output of the generator through tee-joint is connected to the RS. The other arm of the tee-joint is attached to the oscilloscope C1-91. Thus the oscilloscope indicates the superposition of the initial pulse and pulse reflected from the RS. The reflected pulse is shifted by 5 ns with respect to the initial one due to the pulse delay in the cable that connects the RS with tee-joint.

The equivalent circuit of the RS consists of the inductance of the wire that connects the sensor to the coaxial connector and the capacitance that is connected in parallel with the sensor's resistance to prevent the propagation of the microwaves out of the waveguide.

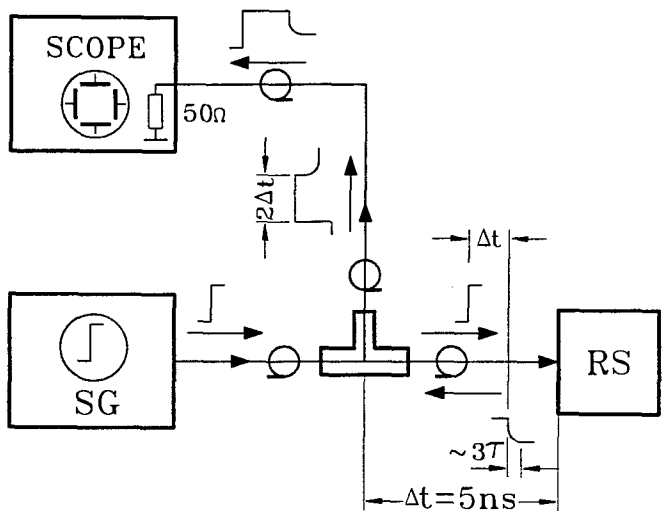

Figure 3. The experimental setup for the RS testing using sub-nanosecond rise time DC pulse generator: SG: DC pulse generator, RS: the resistive sensor under test.

The impedance of the sensor is less than the impedance of the coaxial line (50 Ω) therefore the amplitude of the reflected pulse is negative. Thus, the transient measured by oscilloscope can be related with the response time of the RS.

Measurement of frequency response

The setup for the measurement of the output signal dependence on the microwave frequency is shown in Figure 4. A low-level tunable generator produces microwave pulses that are amplified by a traveling wave tube. The duration of pulses was 1 μs with repetition rate 20 Hz. The maximum pulse power after the amplification was roughly 200 W. A reference pulse power meter with the flat frequency response is connected to the main waveguide through the directional coupler with attenuation 10 dB. It is used for the pulse power control in the main waveguide. Signals from the RS and the reference power meter are measured with oscilloscope Tektronix TDS 520 A.

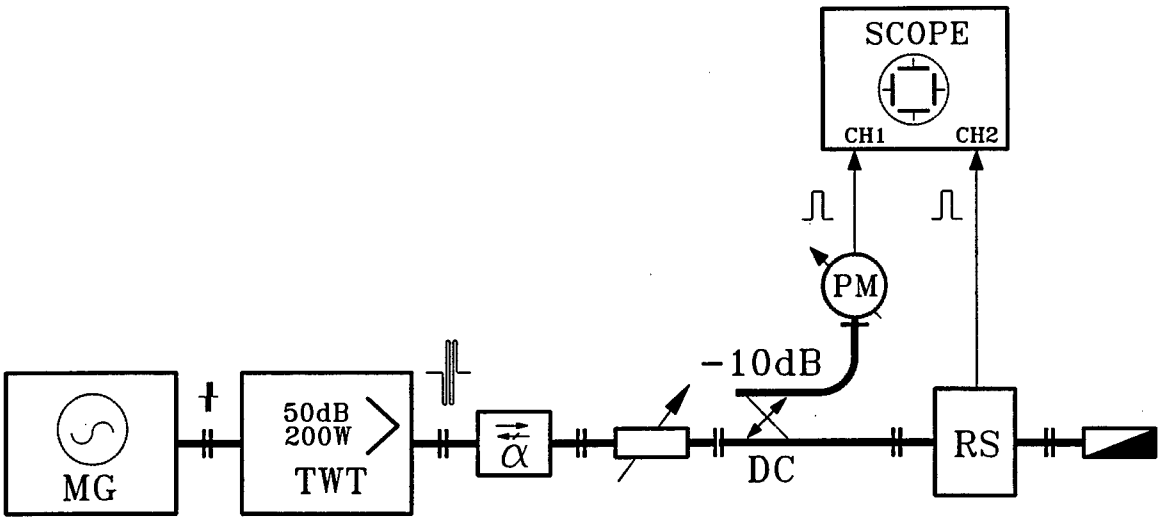

Figure 4. The experimental setup for the frequency response measurement: MG: low level tunable microwave generator, TWT: traveling wave tube, RS: the resistive sensor under test, PM: microwave power meter with known frequency response.

2. DC pulse adapter

The DC pulse adapter is a unit that generates DC pulses for the RS feeding. The circuit that produces delayed synchronizing pulse and the splitting circuit that separates measuring pulse from the feeding one are mounted in it as well.

Since the DC feeding pulse must overlap the microwave pulse, both pulses has to be properly synchronized (Figure 5). The duration of the DC pulse produced by the adapter is roughly 180 μs. So the microwave pulse has to be delayed approximately 150 - 160 μs with respect to the DC pulse. Making use of the adapter it can be done in two ways: using internal synchronizing pulse delay circuit or using external delay of the synchronizing pulse. Both methods of the RS feeding and corresponding diagrams of setup are presented below.

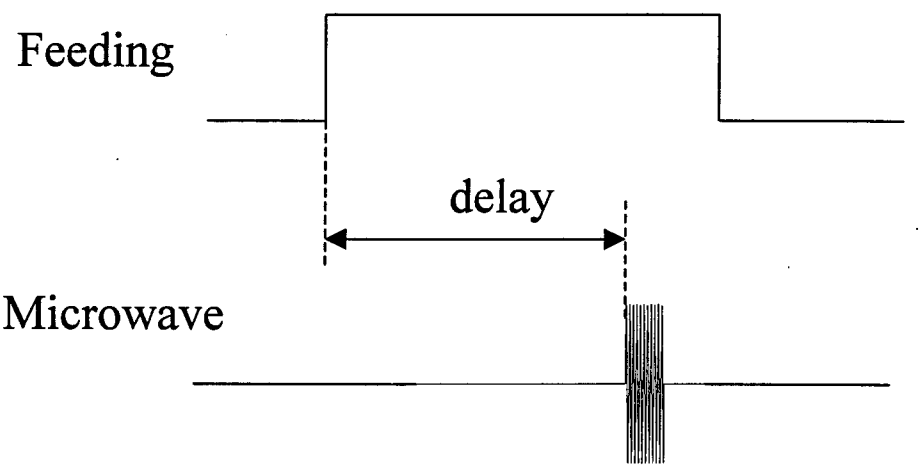

Figure 5. Microwave pulse is delayed in respect of feeding pulse.

Internal delay of the synchronizing pulse

The connections of the adapter with the synchronizing master generator, the high power microwave generator, the sensor and the oscilloscope are shown in Figure 6. The leading edge of the triggering pulse produced by SMG starts the feeding DC pulse. The amplitude and of the feeding DC pulse is 50 V and its duration is roughly 180 μs. After 150 μs the adapter outputs synchronizing pulse for HPMG. Its amplitude is approximately 3 V. The same pulse is used for the oscilloscope triggering. Thus the HPM pulse is delayed in respect to the feeding DC pulse about 150 μs.

External delay of the synchronizing pulse

The measurement can be done using external delay of the synchronizing pulse as well. The connections of cables for this case are shown in Figure 7. The external delay line included in the measurement setup provides that the oscilloscope and the HPMG are triggered after 150 μs when the feeding pulse starts.

Microwave power measurement

Before performing the measurement of the HPM pulse power it is useful to check the delay of the pulse that triggers HPMG and oscilloscope. The pulse has to appear inside two overshoots (closer to the negative one) as it is seen from the oscilloscope view in Figure 6.

When the DC feeding and microwave pulses are properly synchronized the power head outputs the signal. It looks like a short video pulse on the pad of the feeding pulse. The internal differentiating circuit in the adapter cuts the feeding pad and the useful signal together with negative and positive overshoots is transmitted to the

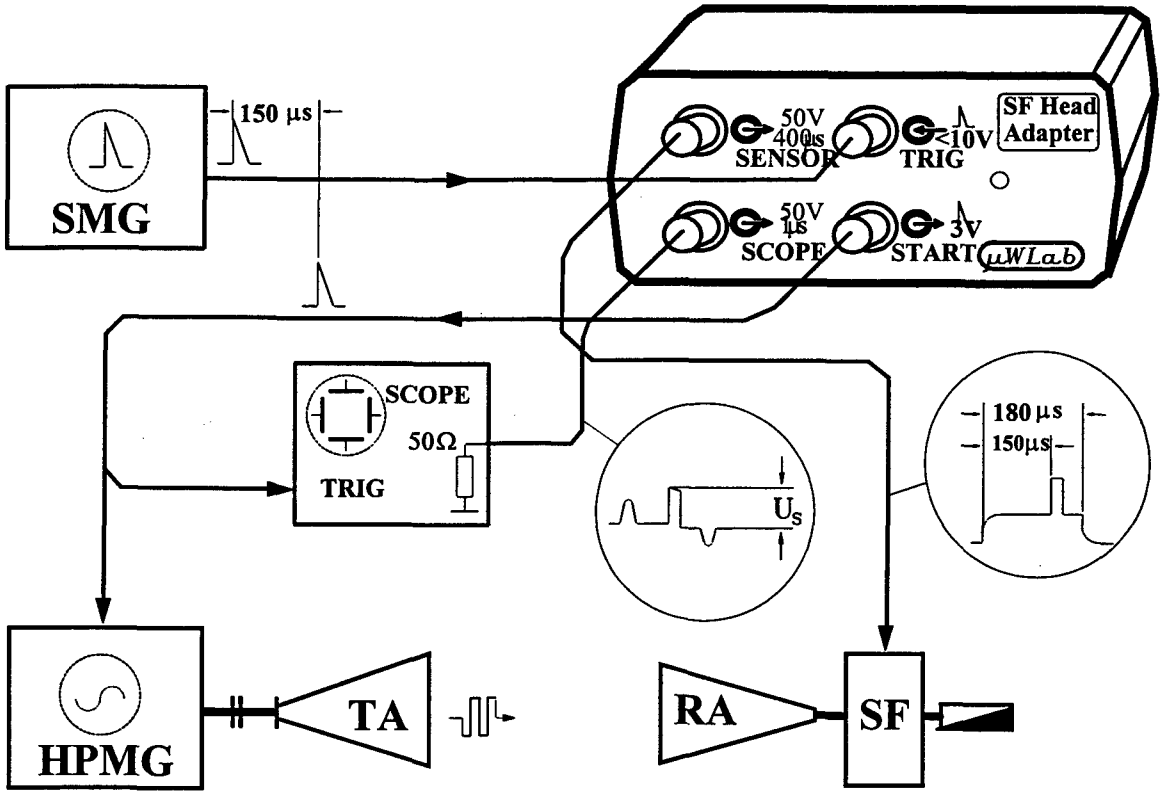

Figure 6. The diagram of the measurement of HPM pulse power density in free space using internal synchronizing pulse delay: SMG: synchronizing master generator, HPMG: high power microwave generator, SF: resistive sensor, TA: transmitting antenna, RA: receiving antenna.

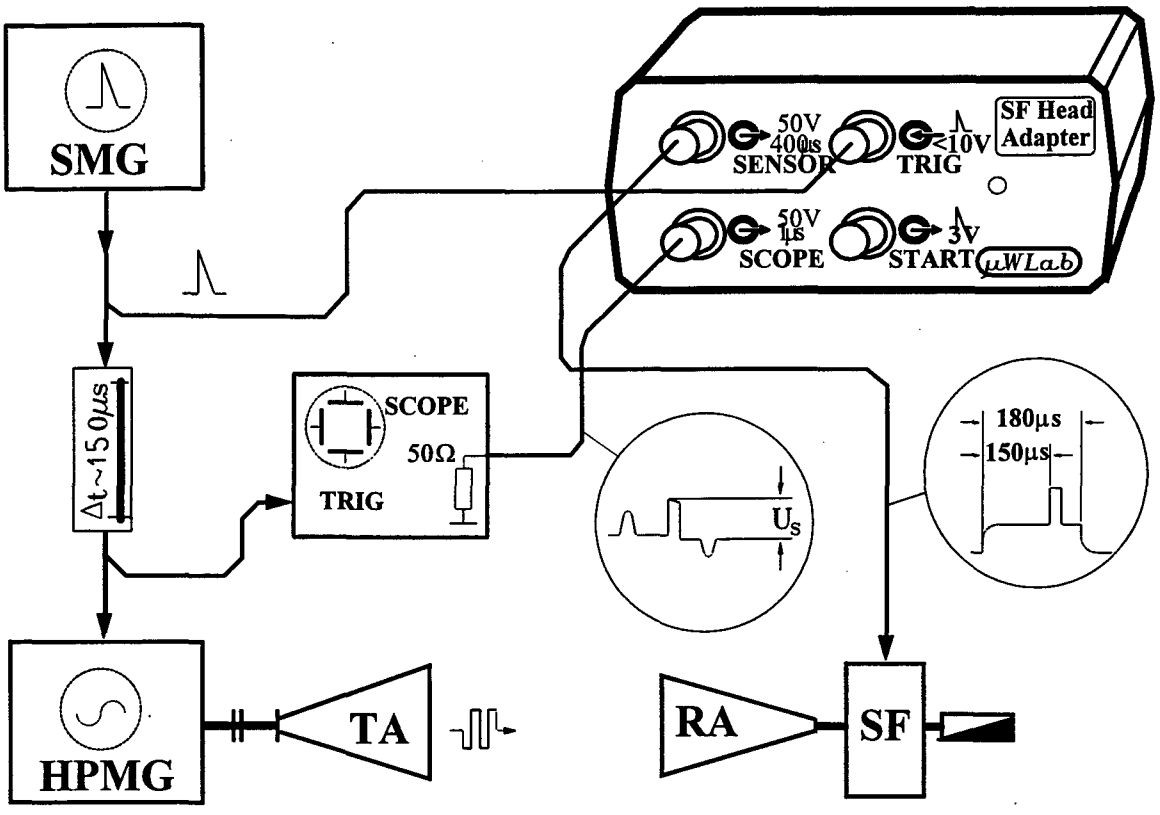

Figure 7. The diagram of the measurement of HPM pulse power density in free space using external synchronizing pulse delay. SMG: synchronizing master generator, HPMG: high power microwave generator, SF: resistive sensor, TA: transmitting antenna, RA: receiving antenna.

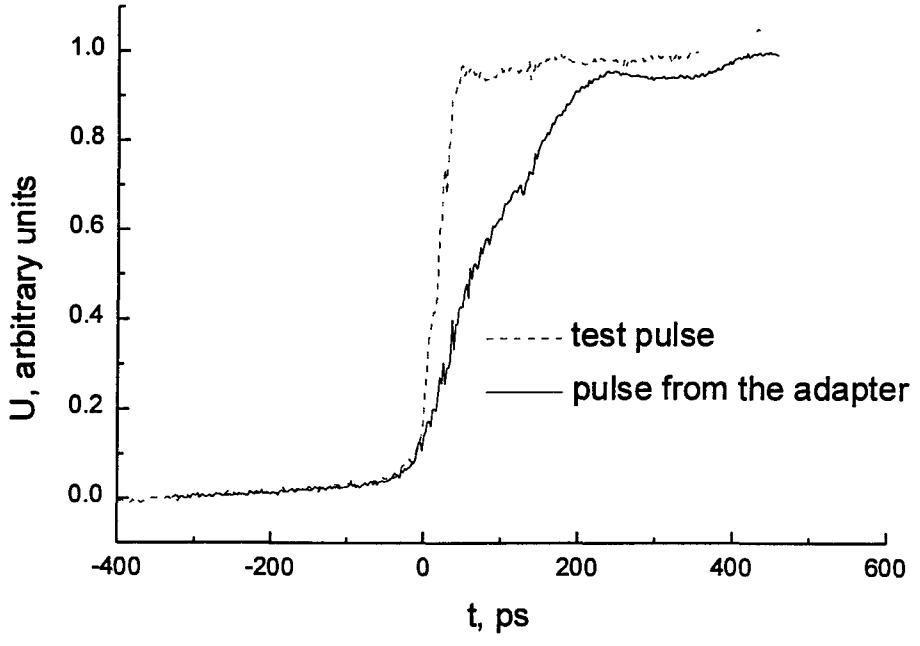

Figure 8. The shapes of the DC test pulse and the pulse from the adapter.

oscilloscope. When the amplitude of the pulse is determined the microwave pulse power can be calculated making use of the calibration curve or the empirical formulae of the particular power head.

Wishing to estimate the distortion of the measuring pulse that is induced by the adapter the test DC pulse with short leading edge was supplied to the sensor connector. The initial test pulse and the pulse from the adapter are shown in Figure 8. It is seen that the rise time of the pulse is roughly 0.2 ns so the distortion of the pulsed should be negligible for the microwave pulse with the duration of a few ns.

The parasitic signal induced in the measurement circuit by the external electromagnetic field might be determined. The sensor's cable has to be disconnected from the adapter and plugged directly into the oscilloscope.

The adapter is not protected against electromagnetic field. So it should not been radiated by HPM. The power switch and AC power supply cable is on the back panel of the adapter.

Technical characteristics of the adapter

1. Amplitude of synchronizing pulse (input)	< 10 V
2. Amplitude of synchronizing pulse (output)	3 V
3. Internal delay (input - output)	150 μs
4. DC feeding pulse amplitude	50 V
duration	180 μs
5. Microwave pulse duration	< 300 ns
6. Connectors	BNC type
7. AC power supply	~ 115 V

3. Characteristics of the resistive sensor

Output signal

The RS for all frequency bands (except L-band) were calibrated using the setup described above. Experimentally determined dependence of the microwave pulse power on the output signal for the particular sensor is fitted by the polynomials. For the RS of S and C-band the microwave pulse power is approximated by the second order polynomial

$$P = A \cdot U_s + B \cdot U_s^2, \tag{3.1}$$

while for the X-band RS the term of 4th order is taken into account

$$P = A \cdot U_s + B \cdot U_s^2 + C \cdot U_s^2. \tag{3.2}$$

The values of the coefficients A, B and C have been determine by fitting (3.1) or (3.2) to the experimentally measured data in a least squares sense. Typical experimentally measured dependencies of the output signal on microwave pulse power together with the calculated one in accordance with (3.1) or (3.2) are shown in Figure 9. Measurements has been performed at a frequency 2.75, 5.7 and 9.3 GHz for S, C and X-band, respectively. As one can see from the figure the largest signal is obtained for the X-band sensor. While the dimensions of the

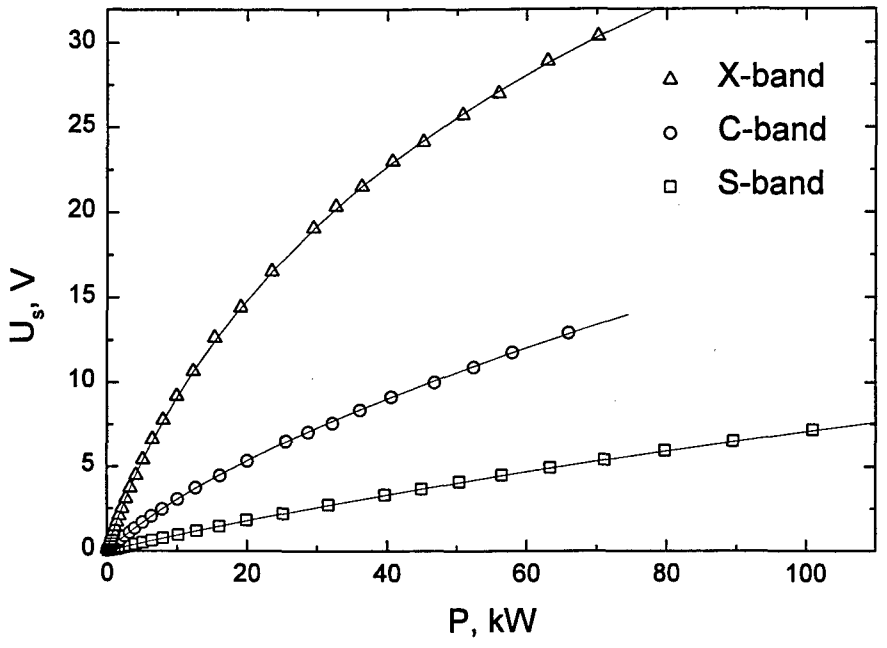

Figure 9. Typical dependencies of the output signal of the RS for different frequency bands on microwave pulse power. Points denote experimental data, solid lines correspond to polynomial fit. Calibration has been done at frequencies: 2.75 GHz (S-band), 5.7 GHz (C-band) and 9.3 GHz (X-band)

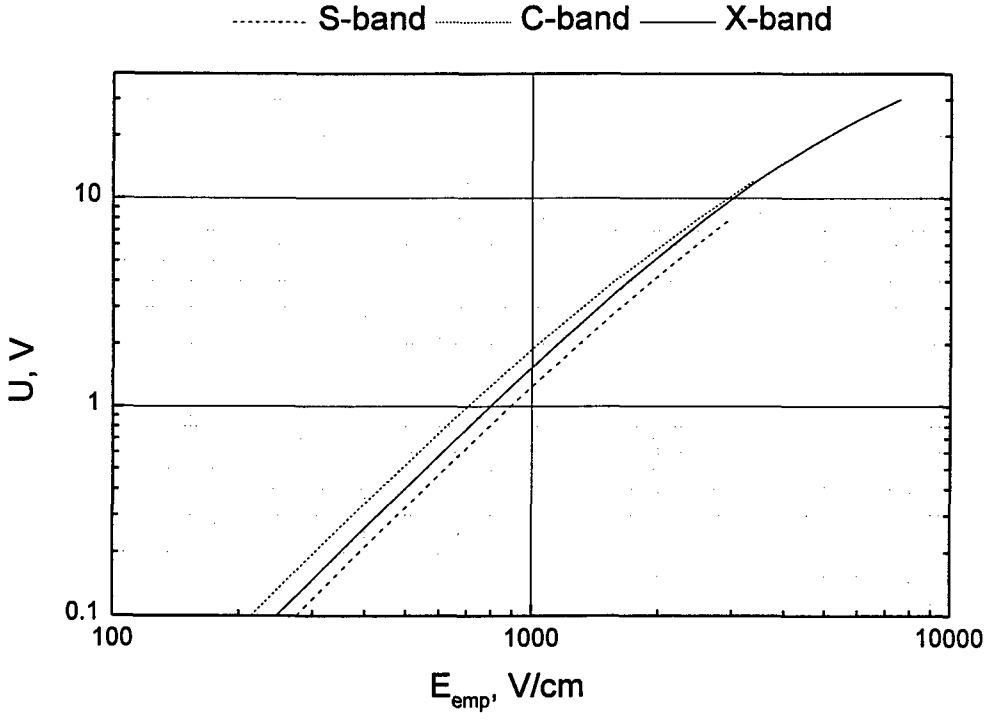

Figure 10. Averaged dependencies of the output signal for the RS of different bands as a function of the electric field strength in the empty waveguide.

waveguide increases the output signal at the same power level decreases significantly. This is not surprising, since the RS is the sensor of microwave electric field rather than the microwave power.

The RS for different frequency bands has been designed increasing the dimensions of the sensor, and the diaphragm proportionally to the waveguide's window dimensions. Doing so, we expect to keep for all band RS the same ratio $k_p=E/E_{emp}$, where E and is the electric field strength in the sensor and empty waveguide, respectively. To verify this assumption the electric field strength in the empty waveguide is calculated at a calibration frequency using well known expression binding electric field strength and microwave power in the waveguide. The dependencies of the output signal as a function of E_{emp} for the S, C and X-band RS are shown in Figure 10. It is seen that the most separated curves in quadratic region differ by factor 1.5. This difference is not so large. Thus, assuming that the output signal of L-band RS depends on E_{emp} in similar way we were able to predict the approximate calibration curve for it.

Frequency response

Frequency response measurements have been done for X-band RS using the setup described in the first chapter. The dependence of the sensitivity on the frequency is shown in Figure 11. As one can see from the figure, the frequency response is practically the same for all investigated RS: The scattering of the absolute value of the sensitivity is less than 30%. The maximum of sensitivity lies around 11 GHz and the maximum to minimum sensitivity ratio in the frequency range 8.2-12.4 GHz is roughly 2.5.

At the beginning of our investigation we had implemented an additional sensor into waveguide to improve the frequency response of the RS. The arrangement of such type RS is shown in Figure 12. It is seen that both sensors: the main that detects microwave pulse power and the additional one, are shifted from the symmetry plane at a distances ΔX_s and ΔX_b, respectively. It was found that the frequency response with the smallest maximum to minimum sensitivity ratio has been obtained when the sensors are shifted at a distance ΔX_s=4 mm, and ΔX_b=8.6 mm. Thus, a few such type X-band RS have been manufactured and tested.

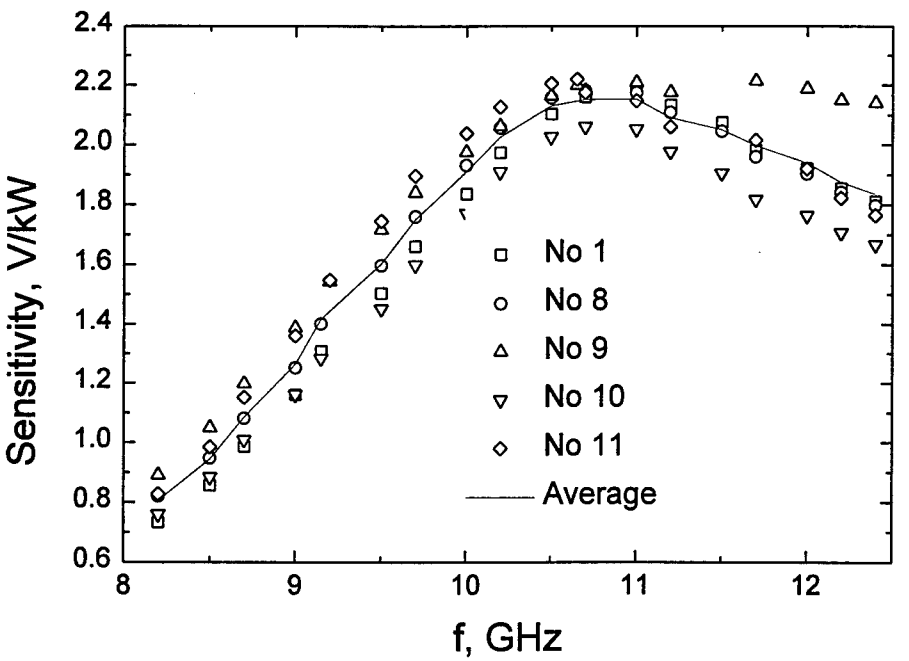

Figure 11. The dependence of the sensitivity on frequency for X-band RS with one sensor placed in the center of broad wall of the waveguide.

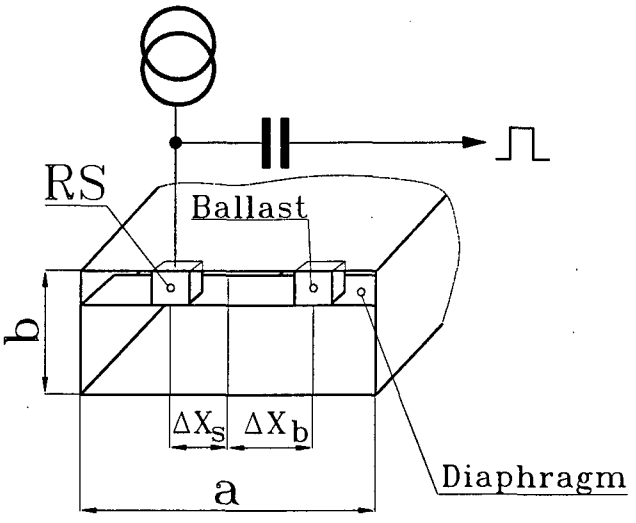

Figure 12. Cross sectional view of the RS with additional ballast sensor for frequency response compensation.

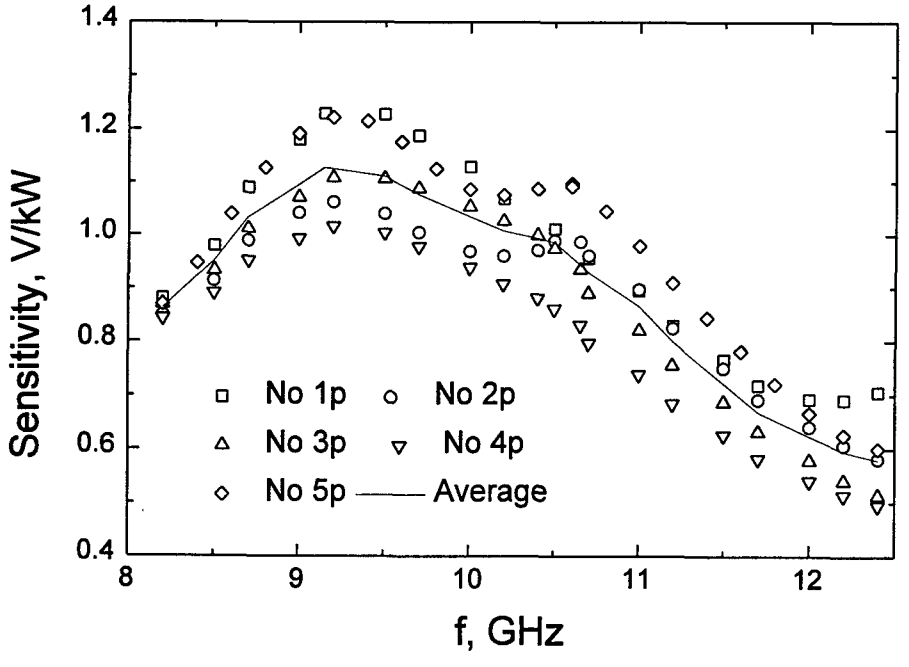

Figure 13. The dependence of the sensitivity on frequency for the RS with additional sensor for frequency response compensation. ΔX_s=4 mm, and ΔX_b=8.6 mm.

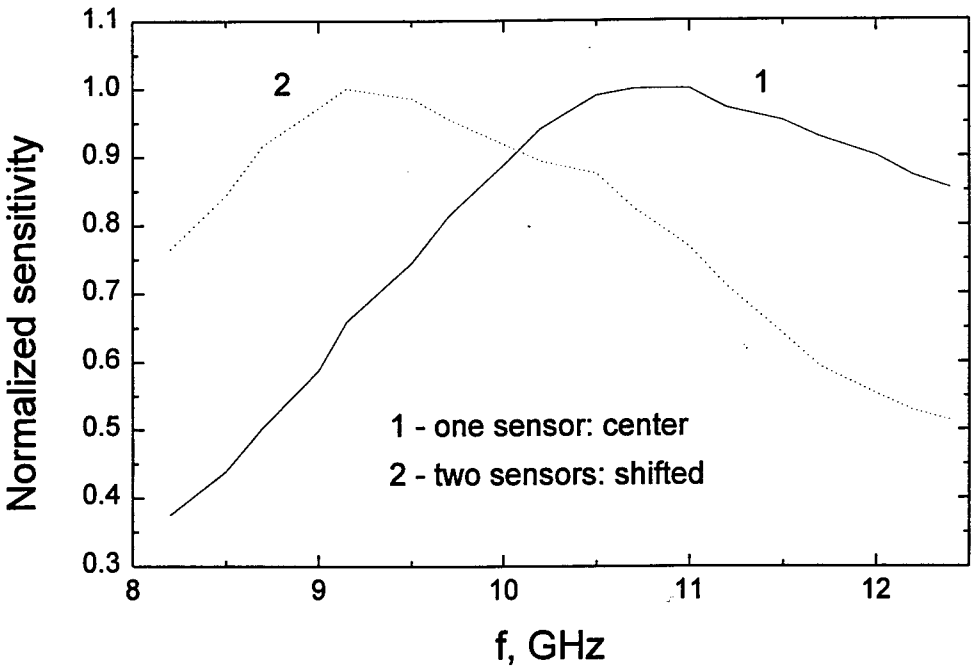

Figure 14. Dependence of normalized sensitivity on frequency for X-band RS. Curve 1 corresponds to the sensor placed in the center of waveguide broad wall, 2 – two sensors shifted at ΔX_s=4 mm, and ΔX_b=8.6 mm from the symmetry plane.

Measured dependencies of the sensitivity versus microwave frequency for the RS with additional sensor are shown in Figure 13. As one can see, the scattering of data is larger in comparison with the RS where only one sensor is employed. The maximum of sensitivity is shifted towards lower frequency (9 GHz). Making use of the additional sensor the maximum to minimum sensitivity ratio decreases and in the frequency range 8.2-12.4 GHz it is less than 2.

As follows from the normalized sensitivity dependencies on frequency shown in Figure 14 two sensor modification is better in the frequency range 8.2 – 11 GHz, while in the frequency range 10 – 12.2 GHz the smaller sensitivity variation for the RS with one sensor is characteristic. Making use of both RS for HPM pulse measurement one can get the sensitivity variation less than ± 12 % in whole frequency range of X-band.

We did not have any powerful tunable microwave sources therefore we can not perform frequency response investigation for S, C and L-band RS. As it was already mentioned, the RS for lower frequency bands has been designed increasing the dimensions of the sensor, and the diaphragm proportionally to the waveguide's window dimensions. Having this in mind, it might be expected that the frequency response of lower frequency RS should be similar to the X-band RS.

Time response

To estimate time response of the RS we used time domain reflectometry method described in the first chapter. Measurement results for different band RS are presented in Figure 15 to Figure 18. As it was mentioned in Chapter 1, the equivalent circuit of the RS consists of the inductance of the wire, the resistance of the sensor and the capacitance that is connected in parallel to the sensor resistance. Analyzing the transients measured for different RS it was realized that the overshoot in the initial part of the transient is mainly conditioned by the wire inductance and/or the mismatch of the impedance of the line that connects the sensor with a coaxial connector. The undershoot observed in the end of transient process is related with the capacitance of the RS. For sake of comparison in each figure the transient measured for ordinary resistor, the resistance of which is equal to the resistance of the sensor, is presented.

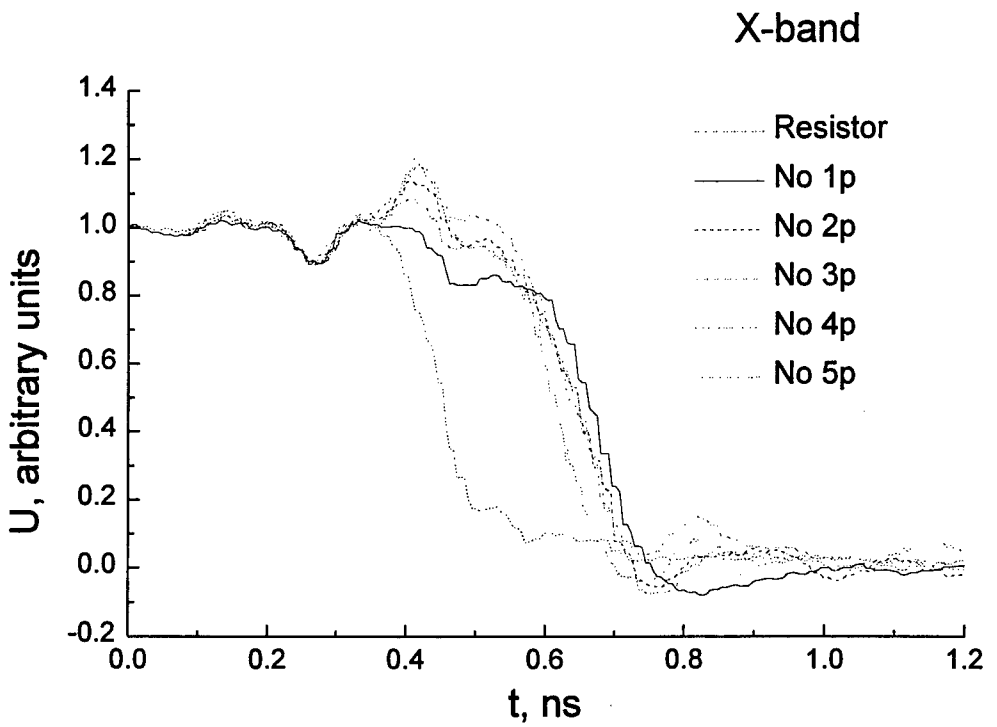

Figure 15. The transients measured for X-band RS.

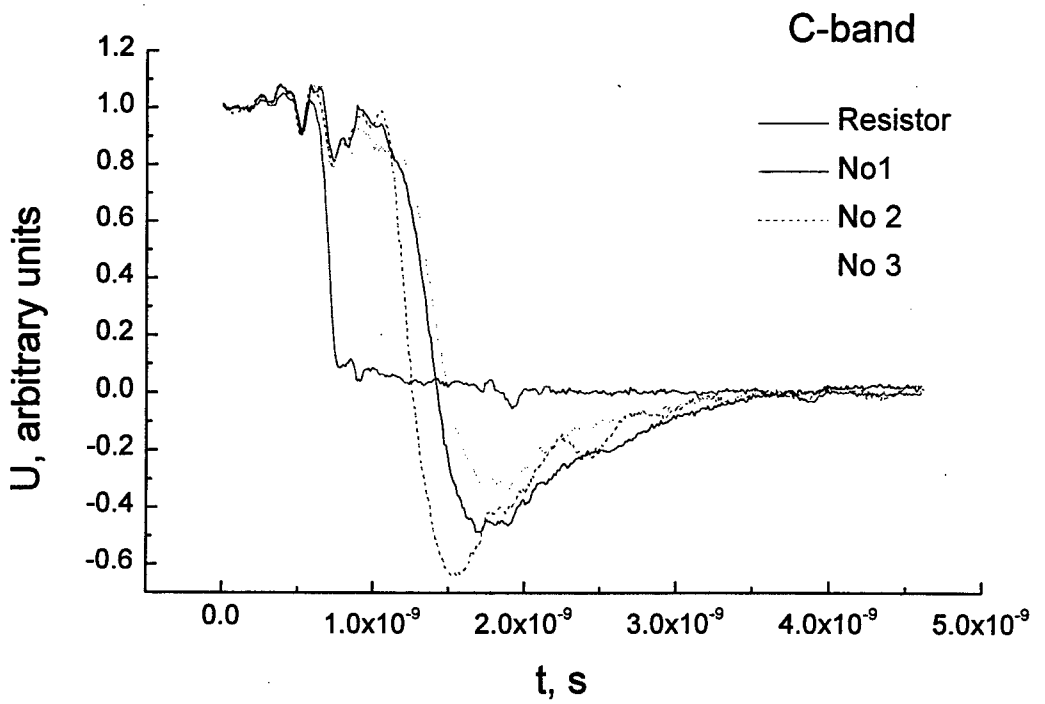

Figure 16. The transients measured for C-band RS.

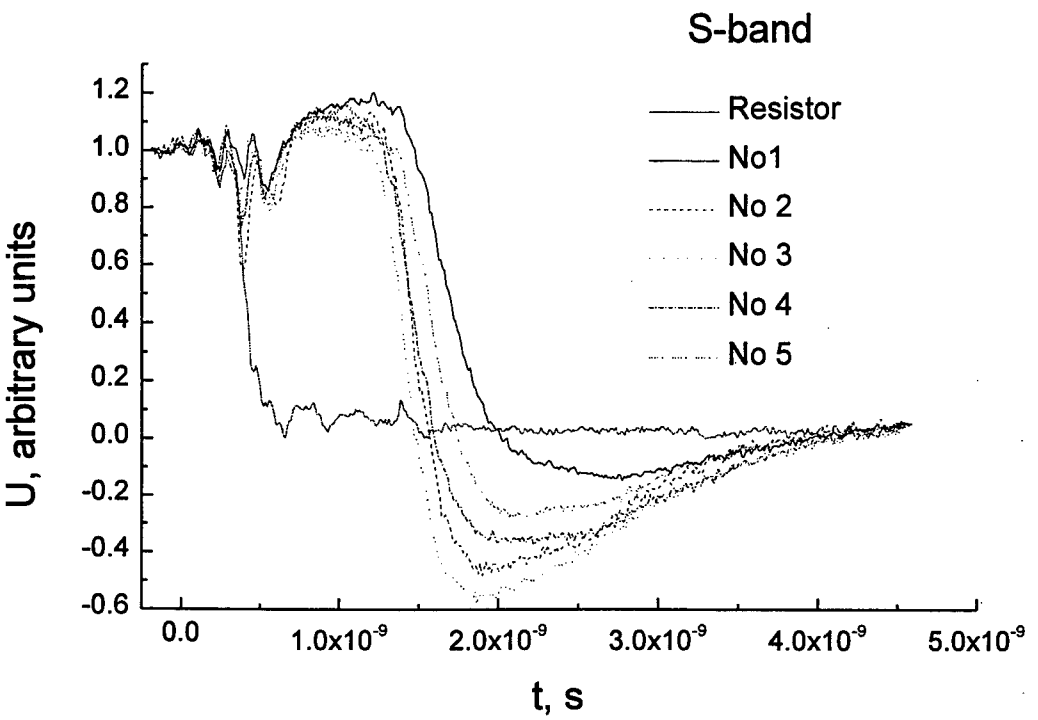

Figure 17. The transients measured for S-band RS.

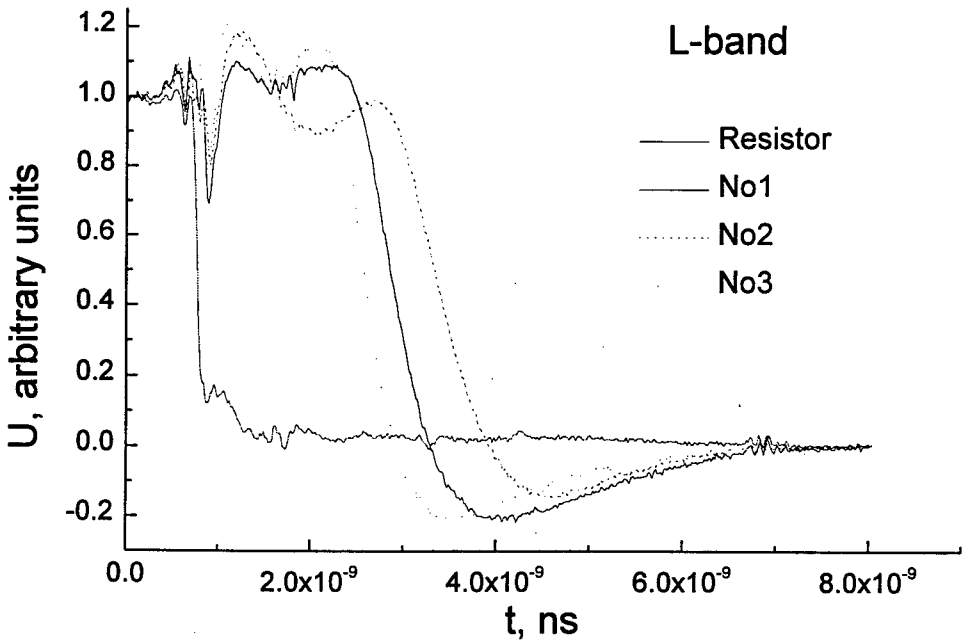

Figure 18. The transients measured for L-band RS.

Assuming that the response time of the RS is roughly equal to the length of the transient process the time responses for the different band RS can be estimated. They are ~0.5 ns for X-band, ~2 ns for C-band, ~3 ns for S-band and ~5 ns for L-band RS. It can be concluded that designed RS is sufficiently fast, since in the worst case they can register HPM pulse power after 10 periods of microwaves for particular frequency band.

Conclusions

1. The RS for HPM pulse measurement in L, S, C and X-bands have been designed, manufactured and tested.
2. The response time of the RS has been estimated using time domain reflectometry method. It was found that the response time for X-band RS is about 0.5 ns.
3. The best maximum to minimum sensitivity ratio less than 2 has been obtained in the frequency range 8.5 - 12.2 GHz for X-band RS with additional sensor.

References

1. M. Dagys, Þ. Kancleris, V. Orševskis and R. Simniškis. "Short high-power microwave pulse measurement using semiconductor resistance change in a strong electric field", Lithuanian Journal of Physics, vol. 36, No. 6, p. 482-485, 1996.

Appendixes

A. Measurements of HPM Pulses at New Mexico University

At New Mexico University measurements of high power microwave (HPM) pulses have been performed using machines SINUS 6 and PI PULSERAD 110A. SINUS 6 produces HPM pulses with peak power about 500 MW, pulse duration ~ 5-7 ns, PI PULSERAD 110A generates 70-100 MW pulses duration of which were in the range 40-50 ns. Carrier frequency was in X-band single shot operation mode is employed. Microwave pulse peak power and pulse shape measured using the RS was compared with the readings from a calibrated crystal detector with short response time (< 1 ns).

Experimental setup is shown in Figure 1A. A HPM source radiates microwaves in to open space. Measuring unit consists of a horn antenna, directional coupler, RS and matched load. It was placed at a distance L from the source and shifted at angle α from symmetry axis of HPM source. The RS directly measures microwave pulse power received by the horn antenna. The adapter that produces DC feeding pulse is connected to the RS via coaxial cable. Microwave power from the directional coupler (20 dB) through the coaxial cable and additional coaxial attenuator feeds the crystal detector. The length of the coaxial cables was about 20 m. The attenuation of microwave in the coaxial cable at a carrier frequency is roughly 10 dB. The crystal detector is calibrated up to 20 mW, thus to decrease power level additional coaxial attenuator is used. Pulse shapes and amplitudes are registered in a screened room by oscilloscope.

Short pulses

To decrease the response time of the RS was one of the main goals has to be achieved improving the

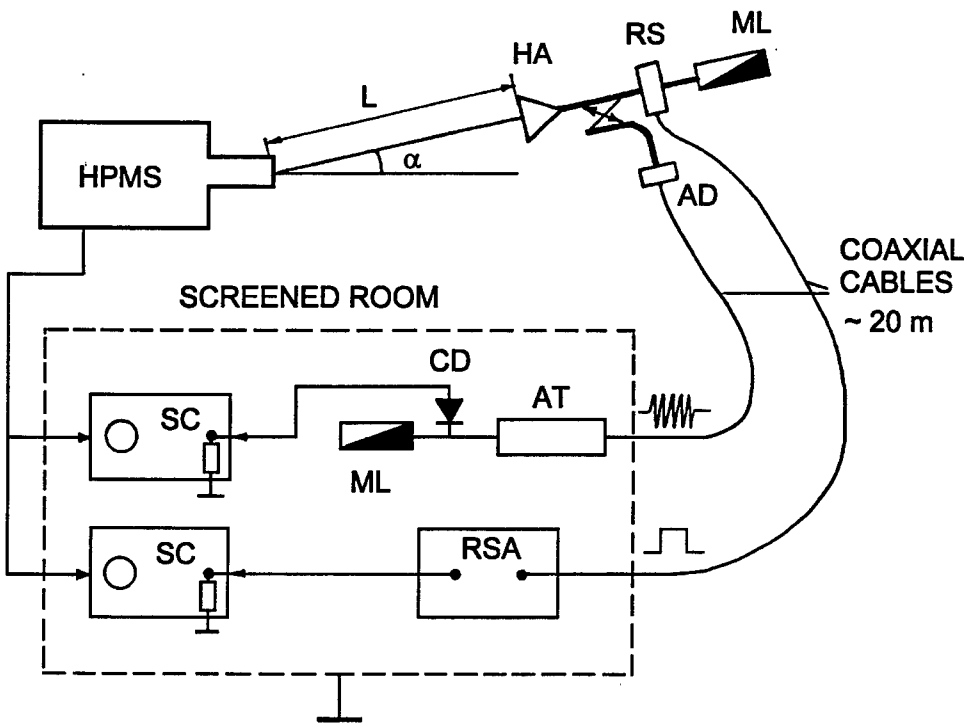

Figure 1A. Experimental setup for HPM pulse measurement: HPMS: high power microwave source, HA: horn antenna, RS: resistive sensor, ML: matched load, AD: waveguide to coaxial cable converter, AT: attenuator, CD: crystal detector, RSA: DC pulse adapter, SC: oscilloscope.

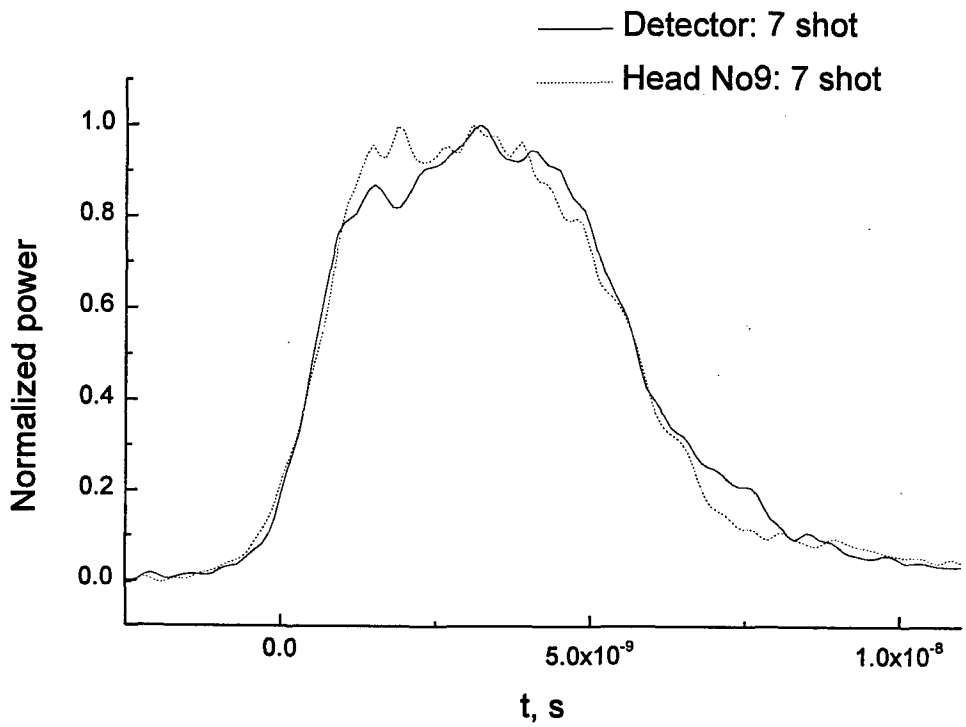

Figure 2A. The shapes of microwave pulses detected by crystal detector and resistive sensor No 9.

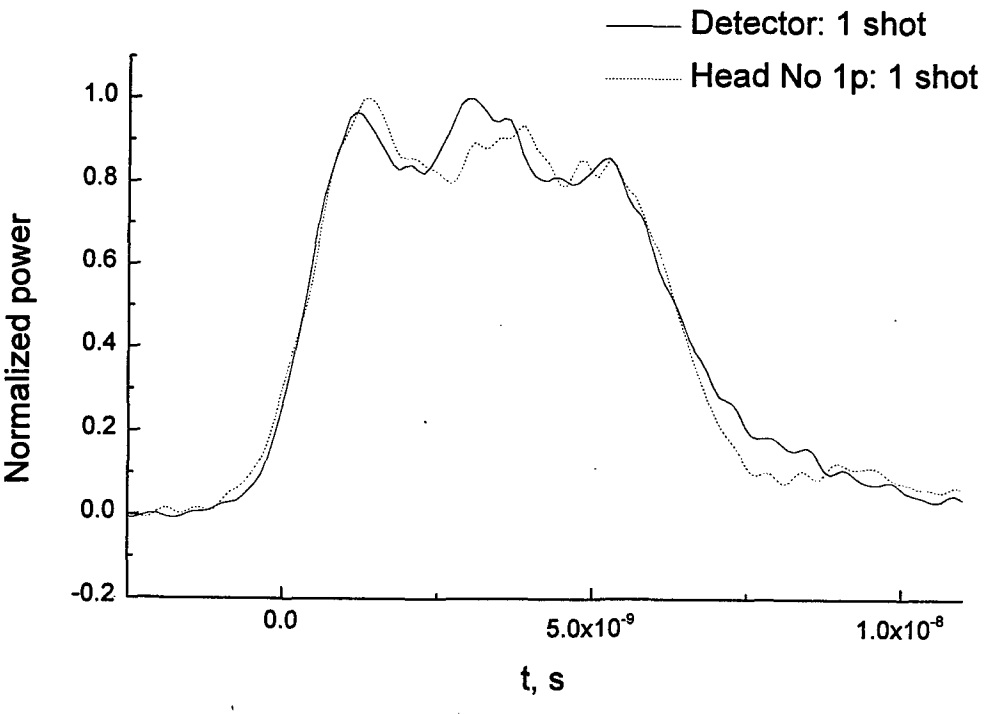

Figure 3A. The shapes of microwave pulses detected by crystal detector and resistive sensor No 1p.

its characteristics. Having no microwave pulse sources with short rise time we estimate the response time of the RS using time domain reflectometry method. It was obtained that the response time of the X-band RS was of the order of 0.5 ns. Nevertheless it is very important to check the estimated rise time of the RS by measuring the response time using short microwave pulses with short rise time.

Thus at the beginning we compare the shapes of the pulses detected by the RS and the crystal detector, the response of which was better than 1 ns. The examples of shapes of pulses are shown in Figures 2A and 3A. The amplitudes of the pulses are normalized to the maximum pulse power detected by the particular device. As one can see from the figures, the shapes of both pulses are practically identical, so it can be concluded that the response time of the RS is not worse than the rise time of the crystal detector.

Comparing pulse power measured by the crystal detector and the RS large difference between readings has been obtained. The RS detects pulse power level in the waveguide that is approximately 4 times lower than the pulse power measured by the crystal detector that is much larger than the calibration error.

Long pulses

In the case of longer pulses generated by machine PI PULSERAD 110a the coincidence between pulse power measured by the crystal detector and the RS is much better. It illustrates data presented in Table 1A. P_d and P_{rs} in the table denote peak pulse power in the waveguide measured using the crystal detector and the RS, respectively. P_{rs}^{*} corresponds to the corrected value of the peak power taking into account the frequency response of the RS. As one can see from the data presented in the table, the RS shows little bit larger values of the peak power but the difference between readings of both devices does not exceed 20%.

The shapes of the pulses detected by the crystal detector and the RS are shown in Figures. 4A and 5A. As one can see from the figures, the pulse detected by the RS is longer from 5 to 7 ns. The difference in pulse length can not be caused by the response time of the RS since it successfully detects shorter pulses and coincidence between shapes was very good (see Figs. 2A, 3A).

It is worthwhile to point out that the carrier frequency increases during the pulse. It may cause some change of the pulse duration when it is travelling in the coaxial cable since the microwave signal attenuation in the cable is roughly 10 dB. To elucidate this point in more detail some additional investigation should be done.

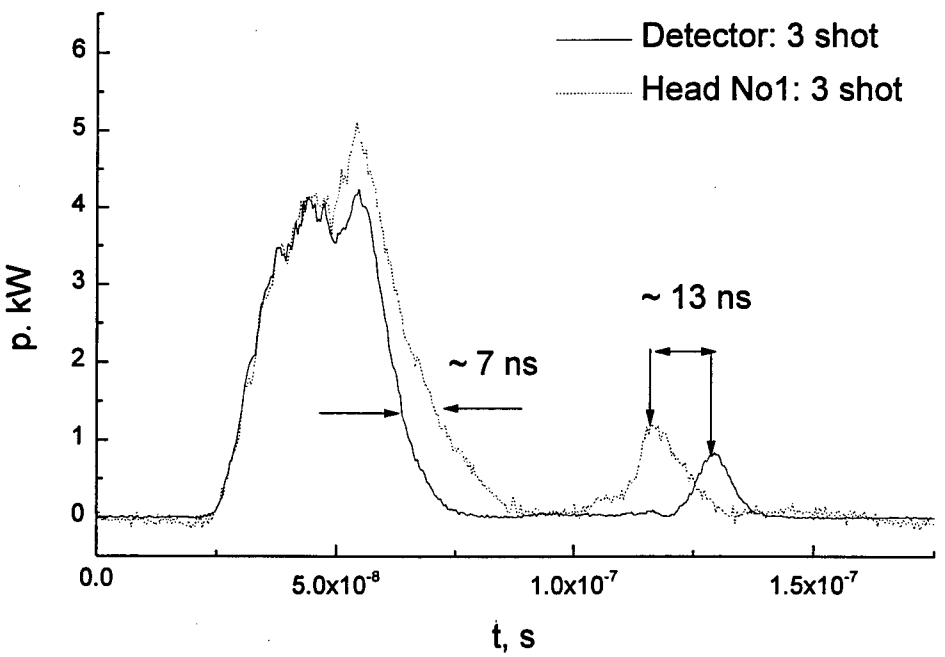

Figure 4A. The shapes of microwave pulses detected by crystal detector and resistive sensor No 1.

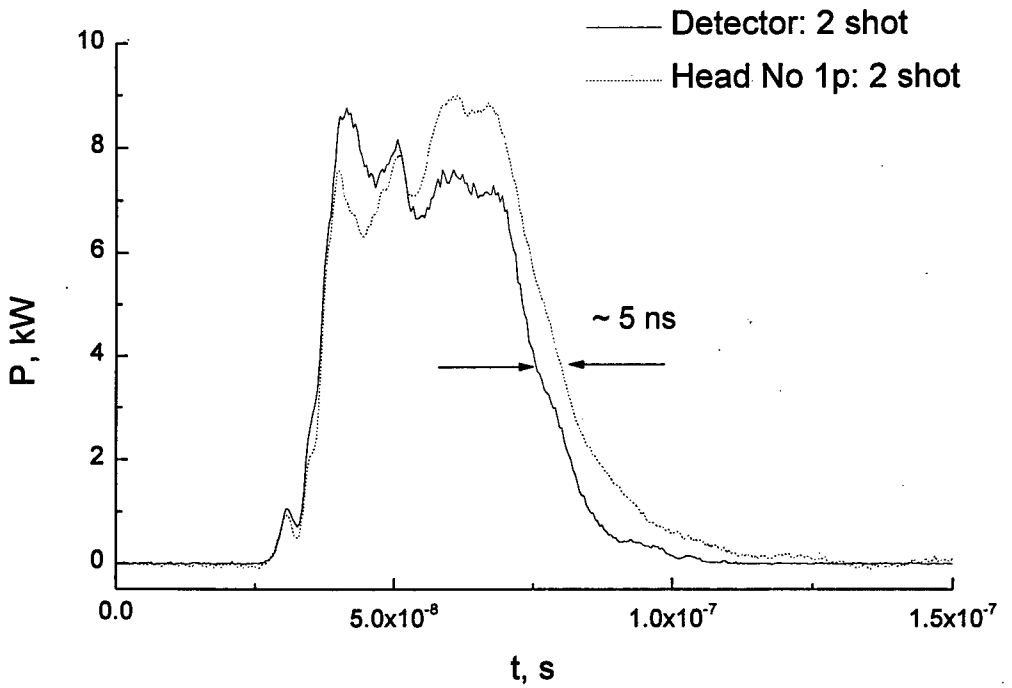

Figure 5A. The shapes of microwave pulses detected by crystal detector and resistive sensor No 1p.

Table 1A. Comparison of peak pulse power measured using the RS and the crystal detector. α=20°, L=104 cm.

Shot No	Freq, GHz	P_d, kW	P_{rs}, kW	P_{rs}^*, kW	P_{rs}^*/P_d
Head No 1					
1	9.30	5.83	5.83	5.83	1.00
2	9.55	5.93	8.37	7.15	1.20
3	9.25	4.25	4.89	5.09	1.20
4	9.25	5.27	5.61	5.84	1.11
Head No 1p					
1	9.25	5.02	5.31	5.31	1.06
2	9.60	8.76	8.76	8.94	1.02
3	9.60	8.78	8.94	9.12	1.04
4	9.25	5.58	5.85	5.85	1.05

Conclusions

The RS has been tested using HPM pulses generated by machines SINUS 6 and PI PULSERAD 110a. Readings of the RS was compared with the readings of the calibrated crystal detector with short rise time (<1 ns). Comparison of the shapes of the short pulses (5-7 ns) has revealed that the rise time of the RS is not worse that the response time of the crystal detector. Reasonable agreement between pulse power levels measured with the RS and the crystal detector has been obtained in the case of longer pulses (40 – 50 ns). Observed shortening of the pulse that is measured by the crystal detector might be caused by the dispersion of microwave pulse with varying carrier frequency in the coaxial line that connects the crystal detector with waveguide.

B. Measurements of HPM Pulses at Cornell University

At Cornell University measurements of HPM pulses have been performed using TWT amplifier at 8.9 - 9.4 GHz. Machine operates in a single shot regime producing pulses up to 150 MW. Their duration is about 100 ns. The output power is transmitted into a coaxial line and absorbed in a dummy load.

Measurement setup is shown in Figure 1B. To control microwave power amplified by TWT an E-probe is inserted in the coaxial line. Its coupling with the coaxial line is 84.5 dB. The E-probe is connected to the ordinary X-band waveguide. Microwave power is transmitted to the screened room via waveguide line. Additional attenuator is used to decrease power level that is measured by a crystal detector. Length of the waveguide is roughly 25 m. Total attenuation of the power transmitted to the crystal detector ranges 114.7 dB. Special directional coupler that connects cylindrical to the rectangular waveguide was designed and fabricated to perform pulse power measurements with the RS. It serves to connect the X-band rectangular waveguide arm with the RS to the main guide. The coupling of the transition is 44 dB. The adapter that produces DC pulses is placed in the screened room and is connected to the RS with a coaxial cable.

Preliminary measurements have revealed that very high noise level is induced in the RS's measuring circuit by electron beam. The amplitude of the noise of the order of 1.5 V is obtained. Making use of double shielded cable and shifting the sensor farther from the main guide (2.2 m), noise level is decreased significantly. Although some oscillations is observed after the end of the measuring pulse the amplitude of which exceeds 200 mV, we were able to perform comparison of power levels registered by the RS and the crystal detector. The results of the measurements are presented in Table 1B. Here U_{rs} and U_d denote the amplitude of the pulse detected by the RS and the crystal detector, P_{rs} and P_d stand for peak pulse power in the main guide measured with the RS and the crystal detector, respectively. P_{rs}^* corresponds to the corrected value of the peak power

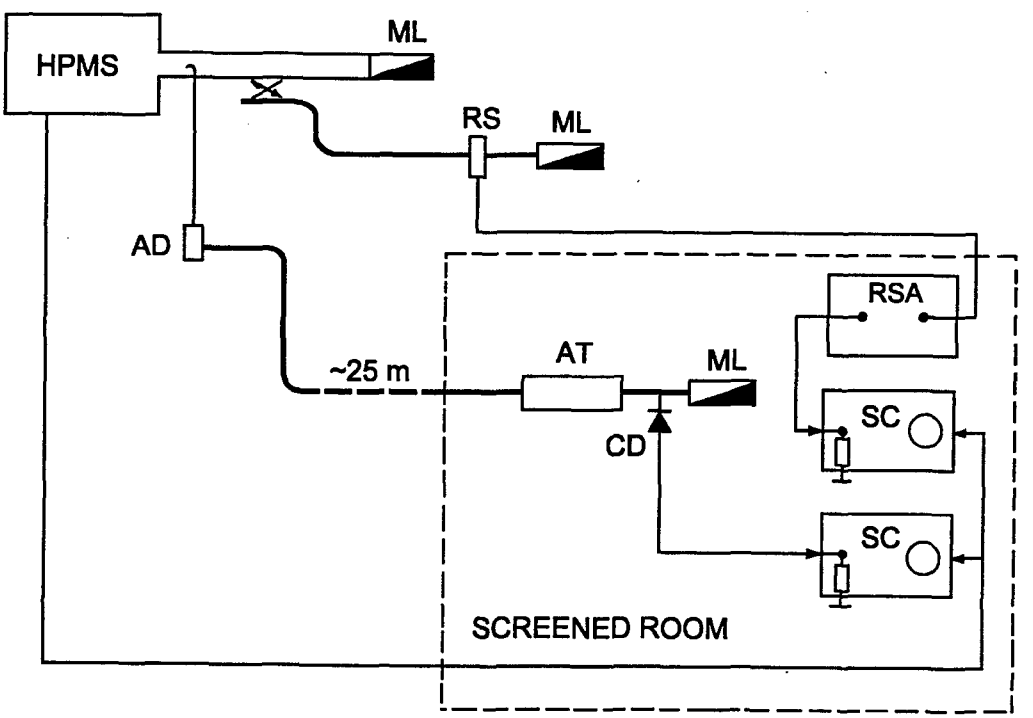

Figure 1B. Experimental setup for HPM pulse measurement: HPMS: high power microwave source, ML: matched load, RS: resistive sensor, AD: waveguide to coaxial cable converter, AT: attenuator, CD: crystal detector, RSA: DC pulse adapter, SC: oscilloscope.

taking into account the frequency response of the RS.

As one can see from the table the difference between readings of the crystal detector and the RS is very large and depends on the frequency. It is difficult to judge what are the reasons of such large difference between the readings of two devices. Concerning the power measured by the RS it is clear that too small coupling between main guide and the RS's arm is employed. The largest peak pulse power measured by the RS does not exceed 1.2 kW. Thus the measured signal is of the order of 1 V and might be significantly influenced by the noise induced in the measuring circuit by the electron beam. The RS is calibrated up to 70 kW. At such pulse power level it can output the signal of the order of 30 V. Thus by increasing the coupling between the main guide and the RS's arm noise to signal ration can be decreased significantly. This in turn should increase the measurement accuracy of pulse power by the RS.

Table 1B. Comparison of peak pulse power measured using the RS (No 10) and the crystal detector.

Shot No	Freq, GHz	U_{rs} V	P_{rs}, MW	P_{rs}^{*}, MW	U_d, mV	P_d, MW	P_{rs}^{*}/P_d
1	9.4	0.88	18.5	17.6	50.0	43	0.41
2	9.3	1.60	34.7	34.7	62.8	54	0.64
3	9.0	1.14	24.3	28.5	4.0	3.4	8.41
4	9.0	0.60	12.5	14.1	18.8	16.2	0.87
5	9.0	1.16	24.7	29.1	10.4	8.0	3.63

Strong dependence of the measured power ratio on the frequency encourage us to perform the additional set of experiments connecting the RS and the crystal detector to the same point of main guide using 44 dB cylindrical to rectangular waveguide coupler. Experimental setup for this case is shown in Figure 2B.

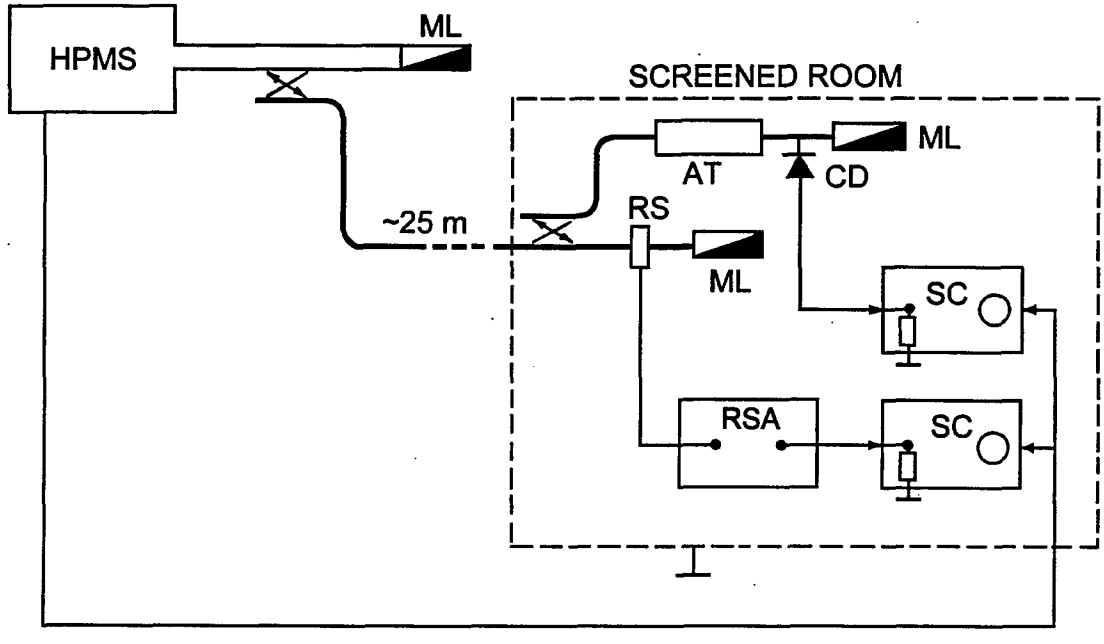

Figure 2B. Experimental setup for HPM pulse measurement when both devices are connected to the same point of the main guide: HPMS: high power microwave source, ML: matched load, RS: resistive sensor, AD: waveguide to coaxial cable converter, AT: attenuator, CD: crystal detector, RSA: DC pulse adapter, SC: oscilloscope.

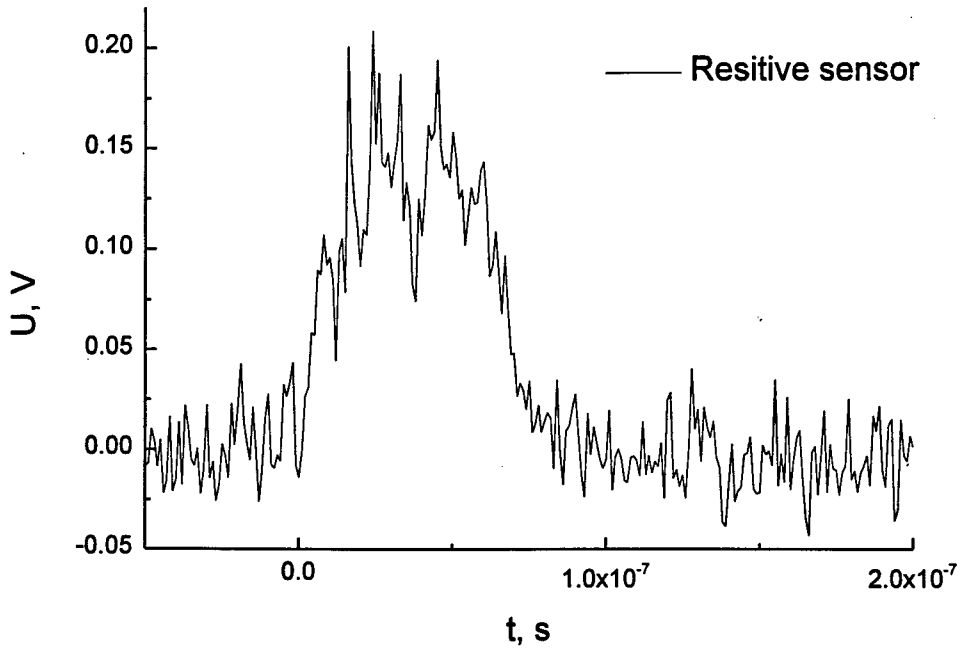

Figure 3B. The shape of the microwave pulse detected by the RS.

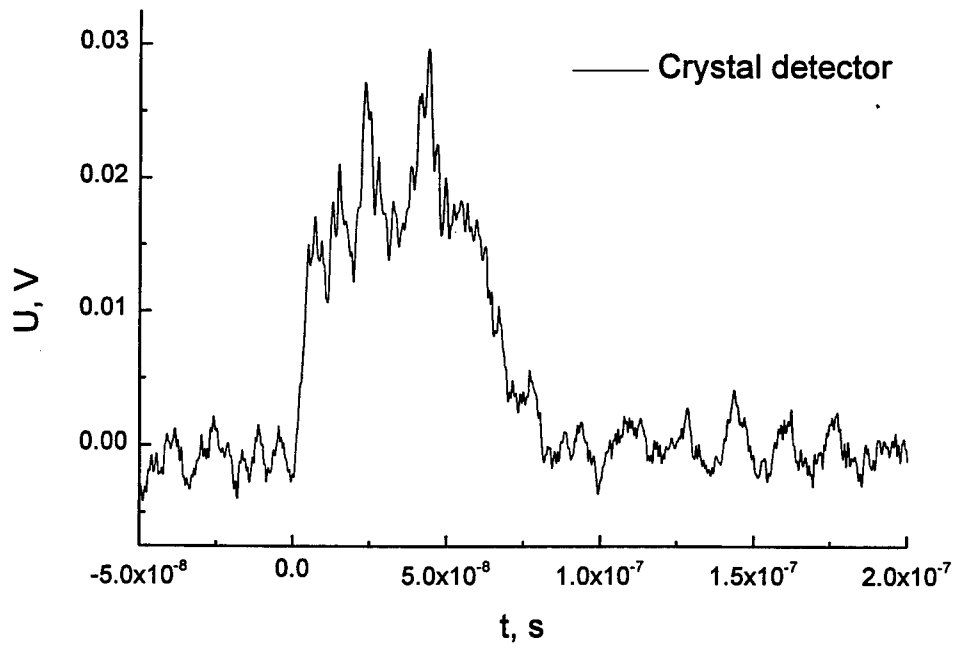

Figure 4B. The shape of the microwave pulse detected by the crystal diode.

Table 2B. Comparison of the peak pulse power measured using the RS (No 10) and the crystal detector.

Shot No	Freq, GHz	U_{rs} V	P_{rs}, MW	P_{rs}^*, MW	U_d, mV	P_d, MW	P_{rs}^*/P_d
1	9.4	0.158	38.1	36.3	21.6	17.9	2.03
2	9.3	0.088	21.2	21.2	12.8	10.6	2.00
3	9.0	0.248	59.6	70.1	42.4	35.1	2.00

Both devices are connected to the waveguide in the screened room. Total attenuation of the microwave power transmitted to the RS and the crystal detector is 55.2 dB and 114.2 dB, respectively.

A few shots have been taken using the setup described above. The shapes of the detected pulses and measurement results are presented in Figures 3B, 4B and Table 2B. As one can see from the figures the shapes of pulses detected by both devices roughly correspond to each other. Noise level induced in the measurement circuits of both devices is essential. As follows from Table 2B the RS shows higher pulse power that differs from the power measured by the crystal detector by factor 2. It is seen that this ratio is practically independent on carrier frequency. Thus the difference between the readings might be caused by the inaccurate estimation of the microwave pulse attenuation (59 dB) in the guide that couples the crystal detector to the waveguide where the RS is connected.

Conclusions

The readings of the RS have been compared with the readings of the crystal detector measuring HPM pulses generated by TWT amplifier. Large scattering of the data has been obtained when the devices were connected to the different points of the main guide. Since the environment nearby microwave source is very noisy the higher power level transmitted to the RS is desirable. When both devices are connected to the same point of the main guide their readings differs by factor 2 but this ratio is independent on the microwave frequency. Since the microwave power passed to the crystal detector is strongly attenuated in comparison with power that is measured by the RS (59 dB), the disagreement in readings might be caused by the error estimating the attenuation of microwaves.

C. Measurements of HPM pulses at Titan Advanced Innovative Technologies

A super–reltron tube at Titan Advanced Innovative Technologies generates hundreds of MW pulse power in the frequency range 800-980 MHz. Although according to the specification L-band RS is devoted for frequency range 1.1-1.4 GHz it was decided to detect envelope of microwave pulse generated by the super-reltron using the RS. The measuring unit is a piece of the waveguide CPR-650 with dimensions of window 82.5x165 mm where the sensor is mounted. The cutoff frequency of the waveguide is 909 MHz, thus the RS can serve as a pulse envelope indicator at the highest frequencies generated by the super-reltron.

The super-reltron outputs power via horn antenna to an anechoic chamber. The RS connected to the dummy load is placed in front of the transmitting horn antenna. There was no horn antenna that matches the dimensions of the waveguide. Therefore the RS's waveguide section by itself serves as a receiving antenna. Since the super-reltron is triggered mechanically by pushing button we can not use DC pulse supply for the RS feeding (microwave pulse has to be delayed about 180 μs in respect of DC pulse that feeds the RS). So for the RS supply 2 V DC voltage source is used. On the wall of the anechoic chamber E-probe is mounted that feeds a crystal detector. The crystal detector, the DC voltage source and the scopes are placed in screened room roughly 30 m apart from the microwave source.

The envelopes of microwave pulses detected by the RS and the crystal detector are shown in Figs. 1C and 2C. The super-reltron generates microwave pulse the duration of which is about 500 ns. Carrier frequency changes during the pulse. Frequency starts at 960 MHz and chirps up to 980 MHz. The change of frequency can be clearly distinguished from the mixer signal shown in Figure 1 (curve 2). The envelopes of microwave pulses shown in Figures 1C and 2C are similar to each other. The maximum amplitude of the pulse obtained from the RS is only 80 mV. It has to be pointed out that the RS used in the experiments is not devoted to detect such low

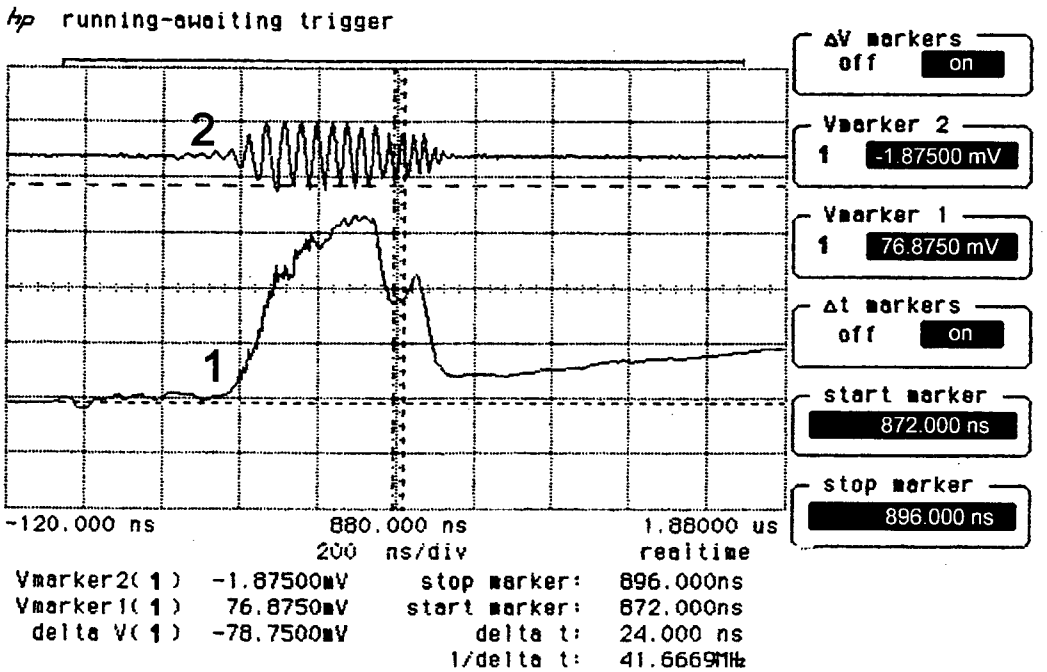

Figure 1C. The shapes of microwave pulse detected by L band RS (1) and the signal from the mixer (2).

frequency. Its sensitivity decreases while the frequency is decreased. The output signal should increase at least 25 times if the DC pulse adapter for the RS supply is used.

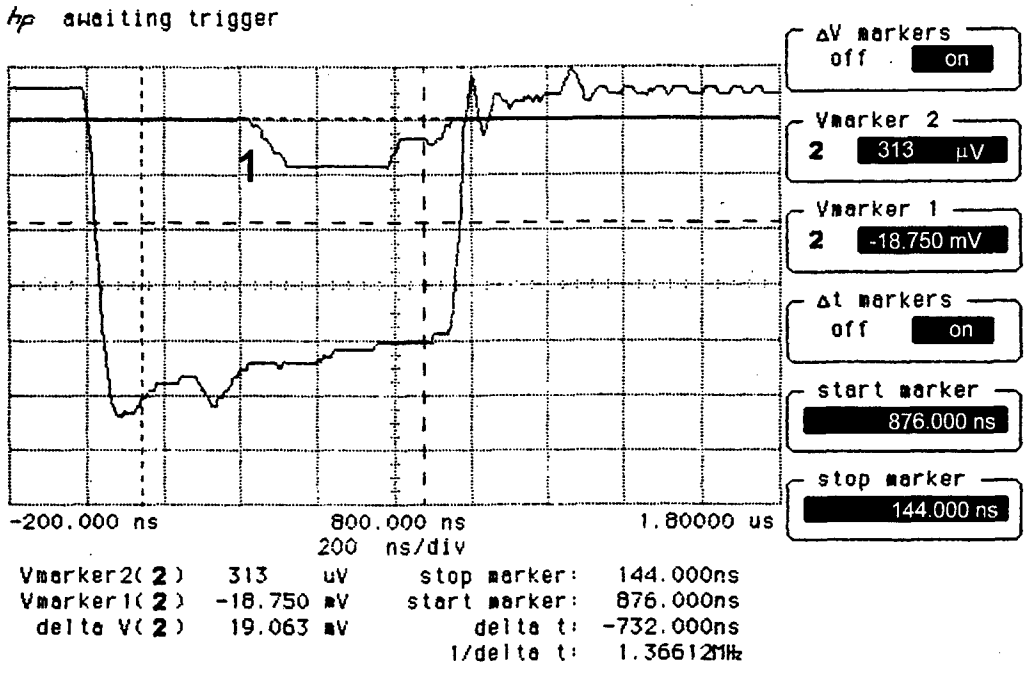

Figure 2C. The shape of microwave pulse detected by crystal detector (1). The same pulse as in Figure 1C.

Conclusions

The L-band RS designed for the frequency band 1.1-1.4 GHz is used to measure the envelope of microwave pulse with carrier frequency in the range 960-980 MHz. The shape of the pulse detected by the RS corresponds to the envelope of the microwave pulse measured by the crystal detector.